

Electronic Supplementary Information

Polarization-insensitive broadband omni-directional anti-reflection in ZnO nanoneedle array for efficient solar energy harvesting

Minjee Ko,^a Hyeon-Seo Choi,^a Seong-Ho Baek^{*b} and Chang-Hee Cho^{*a}

^aDepartment of Emerging Materials Science, Daegu Gyeongbuk Institute of Science and Technology (DGIST), Daegu 42988, South Korea

^bDepartment of Energy Engineering, Dankook University, Cheonan 31116, South Korea

^{*a}Corresponding author, E-mail: chcho@dgist.ac.kr

^{*b}Co-corresponding author, E-mail: seongho@dankook.ac.kr

Contents

Methods

1. Numerical FDTD simulations	3
2. Fabrication of solar cells	5
3. Synthesis of ZnO nanoneedle array	6
4. Characterizations	6
5. Fresnel equation for polarized and unpolarized light	14

Supplementary Figures and Table

Figure S1: Schematic illustration of the FDTD simulation condition	4
Figure S2: Optical constant of ZnO material used for simulation	5
Figure S3: Comparative FDTD simulation study for various geometric parameters of ZnO nanoneedle array	8
Figure S4: Calculated average reflectance values for various incident angles for different heights of ZnO nanoneedle array	9
Figure S5: Calculated reflection and transmission spectral map of ZnO nanoneedle array using FDTD simulation	10
Figure S6: Magnified SEM image of ZnO nanoneedle array	11
Figure S7: Calculated reflectance for SiN _x /planar Si with and without ZnO nanoneedle array	12
Figure S8: Calculated angle-dependent reflection for polarized and unpolarized light using Fresnel equation	13
Table S1: Structural parameters of the ZnO nanoneedle array	4

References	15
------------	----

1. Numerical FDTD simulations

The optical properties of ZnO nanoneedle array were predicted by finite-difference time-domain (FDTD) methods (Lumerical FDTD solutions). The size of FDTD simulation region in x-y plane is $0.05 \times 0.05 \mu\text{m}^2$, which is same with diameter and period of ZnO nanoneedle array. The Bloch boundary condition was used in the x- and y-directions to realize the two-dimensional periodic array. Also, the stretched coordinate perfectly matched layer (PML) was set along the z-direction to remove reflected light waves from the simulation boundary. The dispersive refractive index of ZnO was taken from PV Lighthouse library (Figure S2) and those of other materials (Si and SiN_x) were based on Lumerical materials database [1]. The mesh size was set as 1 nm along x, y, and z directions for the calculations. In order to obtain the angle-dependent characteristics, we used the plane wave with broadband fixed angle source technique (BFAST) which enables us to calculate simulation results at specific incident angles. The range of incident angles was varied from 0 to 64° by step of 2° . Structural parameters of ZnO nanoneedle array were set to be 230 nm in height, 50 nm in diameter, and 50 nm in period (Table S1). A schematic illustration of the detailed simulation set-up is shown in Figure S1.

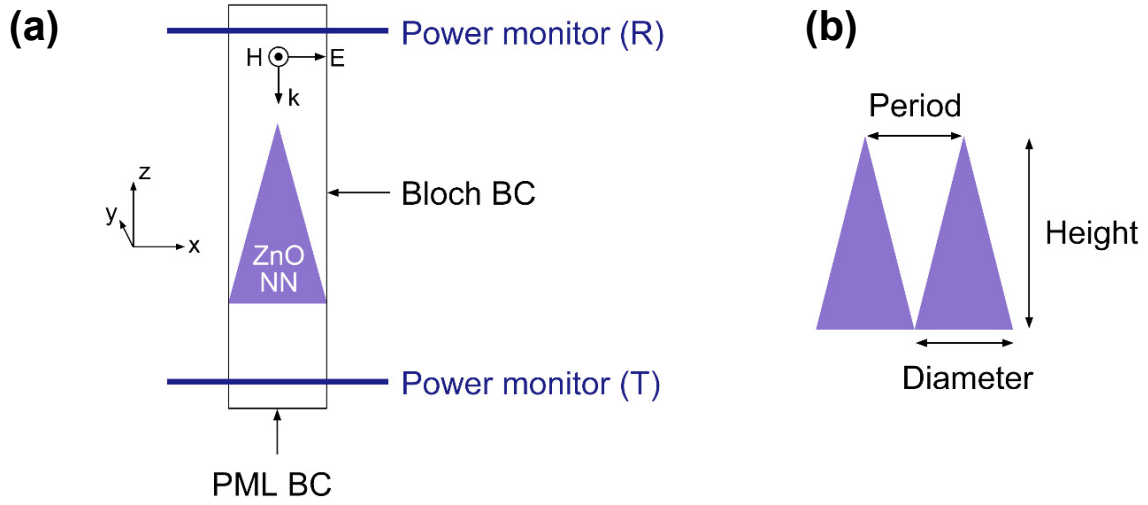


Figure S1. (a) Schematic illustration of the FDTD simulation condition. The black rectangular line indicates the simulation region. The Bloch boundary condition (BC) was used in the x- and y-direction to realize the two-dimensional periodic array. The perfectly matched layer BC was set along the z-direction to exclude the reflected light waves from the simulation boundary. The propagation direction (k) and electric field are lie on the z- and x-axis, respectively. The power monitor (for reflection (R) and transmission (T)) is placed as shown in image. (b) The structural parameters of the ZnO nanoneedle array, as shown in Table S1.

Table S1. Structural parameters of the ZnO nanoneedle array

Height	Diameter	Period
230 nm	50 nm	50 nm

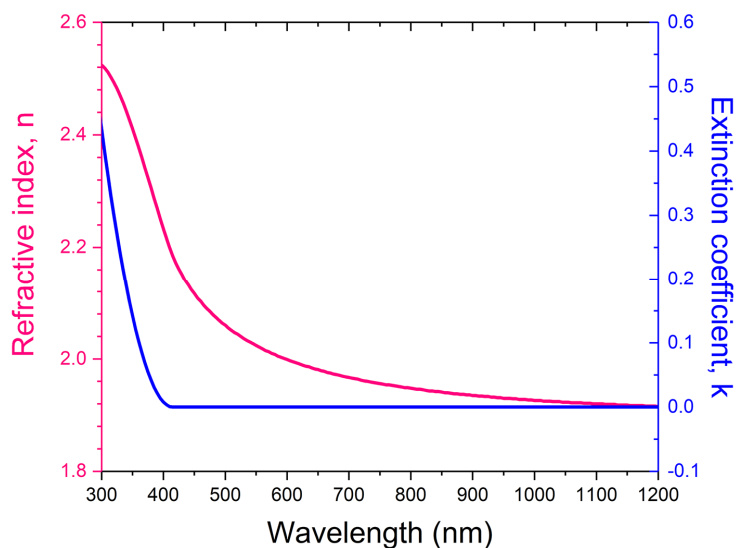


Figure S2. Optical constant of ZnO material. The pink and blue solid lines indicate the refractive index (n) and extinction coefficient (k), respectively. The dispersive refractive index of ZnO was taken from PV Lighthouse library [1].

2. Fabrication of solar cells

p-type Si wafers with a resistivity of 5-10 ohm-cm and (100) crystal orientation were used as a substrate. The Si wafers were cleaned using a piranha solution ($\text{H}_2\text{O}_2 : \text{H}_2\text{SO}_4 = 1 : 3$) at 120 °C for 30 min. Using ion implantation processes with an energy of 50 keV, the n^+ - and p^+ -regions were defined on the top and bottom of Si substrate, respectively. Phosphorus and boron atoms were used as dopants with concentration of 2×10^{15} and 1×10^{15} atoms/ cm^3 , respectively. Subsequently, the rapid thermal annealing was conducted at 1050 °C for 2 min for dopants activation. In order to remove the native oxide and oxide layer formed on the surface of Si wafers during annealing process, the fabricated samples were immersed in the buffered oxide etch (BOE) solution for 3 min and then rinsed thoroughly with deionized (DI) water. To form an anti-reflection layer, 100-nm-thick SiN_x was deposited on the top of the Si substrate using plasma enhanced chemical vapor deposition (PECVD). An electrode pattern was defined on the top of the n^+ -region by photolithography. In order to secure the contact area of electrode, the patterned SiN_x was etched by BOE for 10 min and then rinsed with DI water. Then, Ohmic contacts were formed for the top and bottom electrodes using Ti/Au (50/100 nm) and Al (300

nm) by e-beam evaporator, respectively.

3. Synthesis of ZnO nanoneedle array

ZnO nanoneedle array was synthesized using a two-step method. First, the ZnO seed solution was obtained by a well-established method [2]. The ZnO seed solution was prepared by dissolving zinc acetate dehydrate of 0.3 M ($\geq 99\%$, Aldrich) in 2-methoxyethanol (anhydrous, 99.8%, Aldrich). After stirring the solution at room temperature for 2 h, ethanolamine of 0.3 M ($\geq 99\%$, Aldrich) was subsequently added to the solution and stirred at 60 °C for 1 h. The surface of SiN_x/planar Si solar cells was pretreated with O₂ plasma to form a hydrophilicity, then the ZnO seed layer was coated on the surface of solar cells by solution coating process with the spin speed of 4000 rotations per minute (rpm), followed by annealing at 175 °C for 10 min. Second, the ZnO nanoneedle arrays were grown by a hydrothermal method [3]. The growth solution of ZnO nanoneedle arrays was prepared using zinc nitrate hexahydrate (0.025 M) and hexamethylenetetramine (HMTA; 0.025 M) in DI water of 300 ml. To obtain a tapered shape of ZnO nanoneedle, 1,3-diaminopropane of 120 mM (DAP; 99%, Aldrich) was added to the growth solution for pH control and stirred for 30 min. The ZnO seed layer coated SiN_x/planar Si solar cell was placed upside-down in the growth solution and the ZnO nanoneedles were grown on the seed layer at 85 °C for 50 min in oven.

4. Characterizations

The morphological features of the fabricated ZnO nanoneedle array were measured by high resolution field emission scanning electron microscope (FESEM, SU8020, Hitachi). To obtain the optical properties of the ZnO nanoneedle array, the reflectance measurements were performed using a UV-Vis-NIR spectrophotometer with an integrating sphere (Cary 5000, Agilent). The incident angle-dependent photocurrents of solar cells were characterized using a photocurrent measurement system, in which the incident angle of laser light (450 nm wavelength) can be tuned by a goniometer. The laser beam shape was elliptical with the minor axis of 2.5 mm and major axis of 3 mm at normal incidence. The photocurrent was measured

for both TE- and TM-polarizations. The power conversion efficiency of solar cells was measured under 1 sun illumination (100 mW/cm^2) using a solar simulator (WSX-1555S-L2, Wacom, AM 1.5 G) with a source meter (2400, Keithley). The external quantum efficiency was obtained from a spectral response measurement system (CEP-25BX, Jasco).

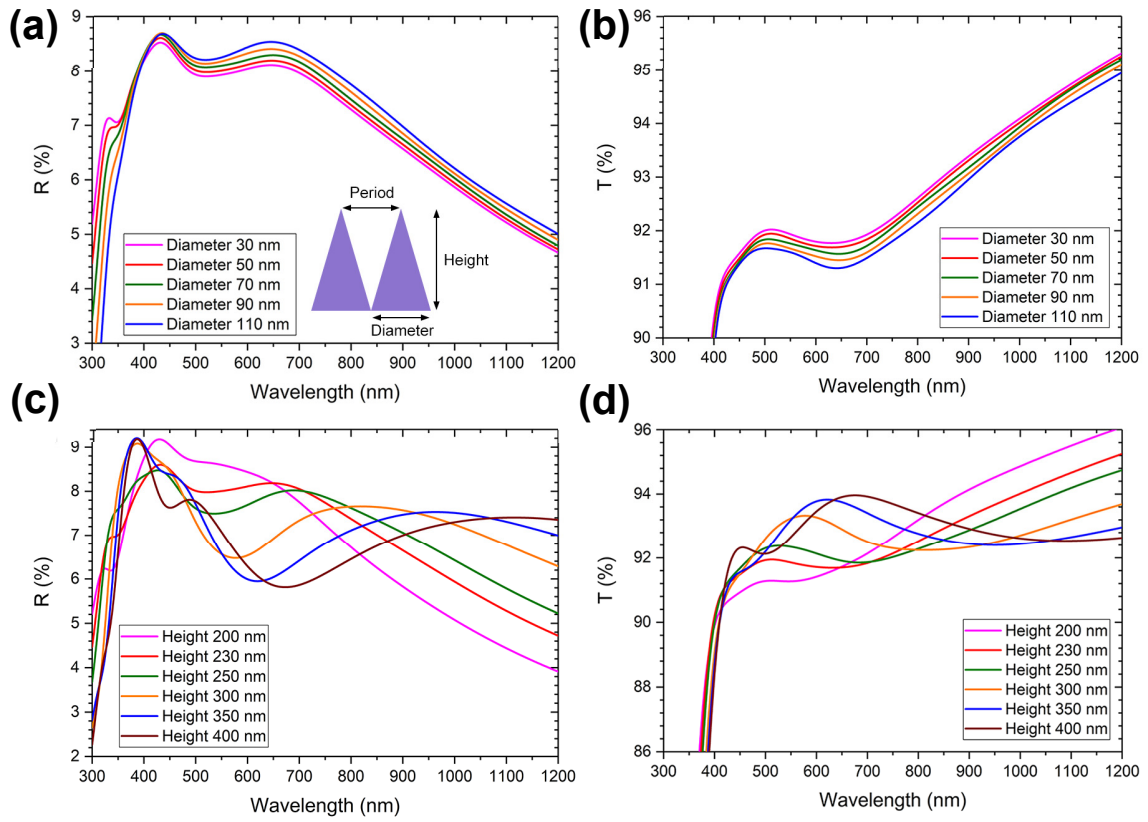


Figure S3. (a to d) Comparative FDTD simulation study for various geometric parameters of ZnO nanoneedle array at normal incidence. Calculated diameter-dependent reflection (a) and transmission (b) spectra. The height was fixed as 230 nm. The period is the same with the diameter to realize the two-dimensional periodic array. The inset of Fig. S3(a) shows the definition of geometric parameters of ZnO nanoneedle array. Calculated height-dependent reflection (c) and transmission (d) spectra. The diameter and period were fixed as 50 nm.

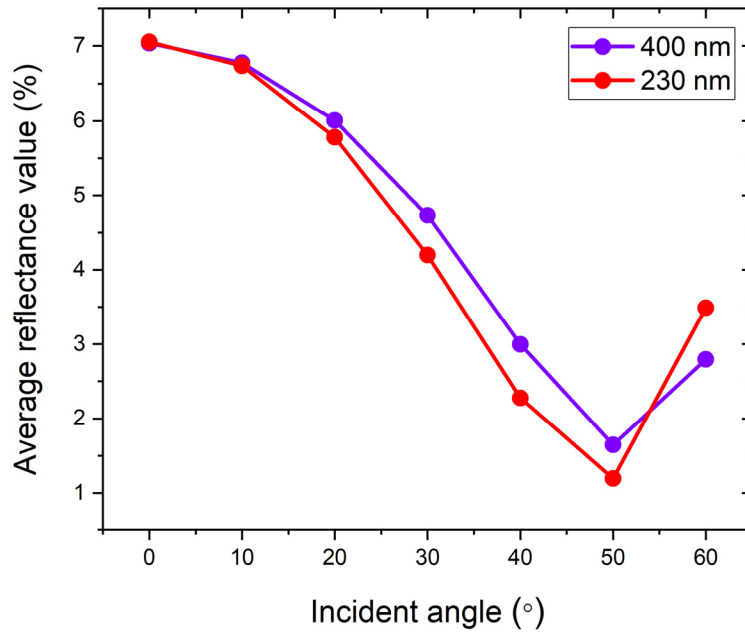


Figure S4. Calculated angle-dependent average reflectance values for the different heights of ZnO nanoneedle array. The average reflectance values were obtained from calculated incident angle-dependent reflection spectra over the spectral range of 380 to 1200 nm. For the incidence angles from 0° to 60°, the average reflectance value for the height of 230 nm is ~4% lower than that of 400 nm.

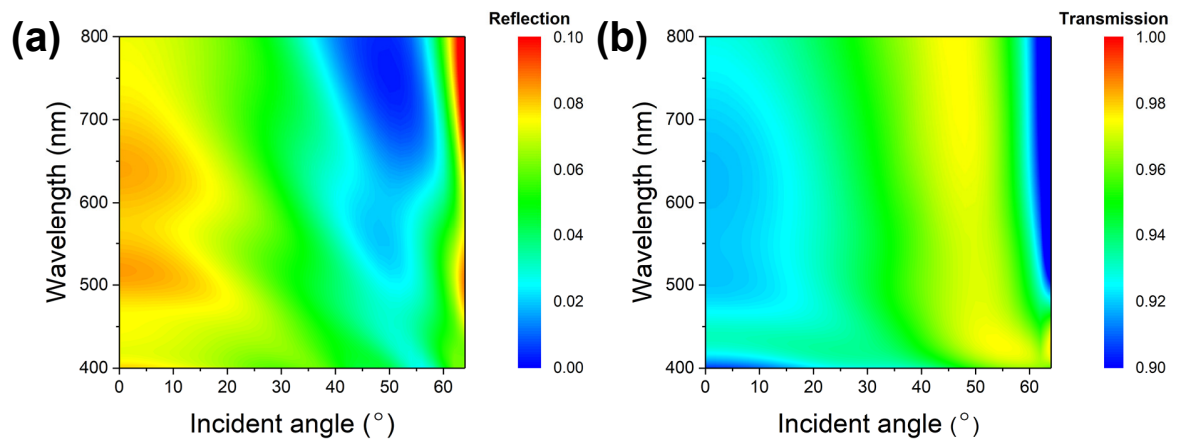


Figure S5. (a and b) Calculated reflection (a) and transmission (b) spectral maps of ZnO nanoneedle array using FDTD simulation as a function of the wavelength and incident angle. The results are identical with Figure 1(b) and (c) of the main text, but the scale of intensity has been adjusted for the visibility.

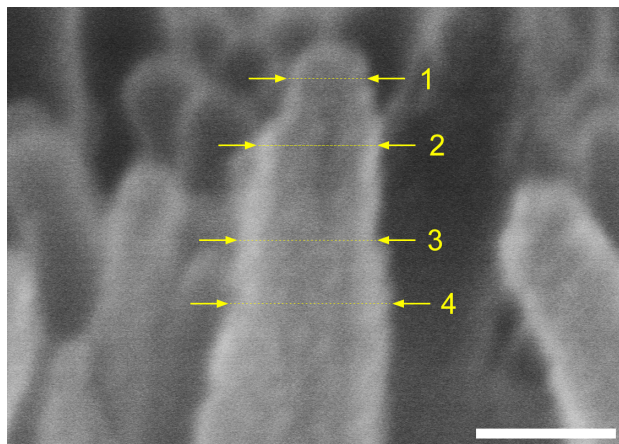


Figure S6. Magnified SEM image of the tip area of ZnO nanoneedle. The numbers indicate the positions where the diameter is measured to be 26, 39, 46, and 52 nm at the position 1 to 4, respectively. The scale bar is 50 nm.

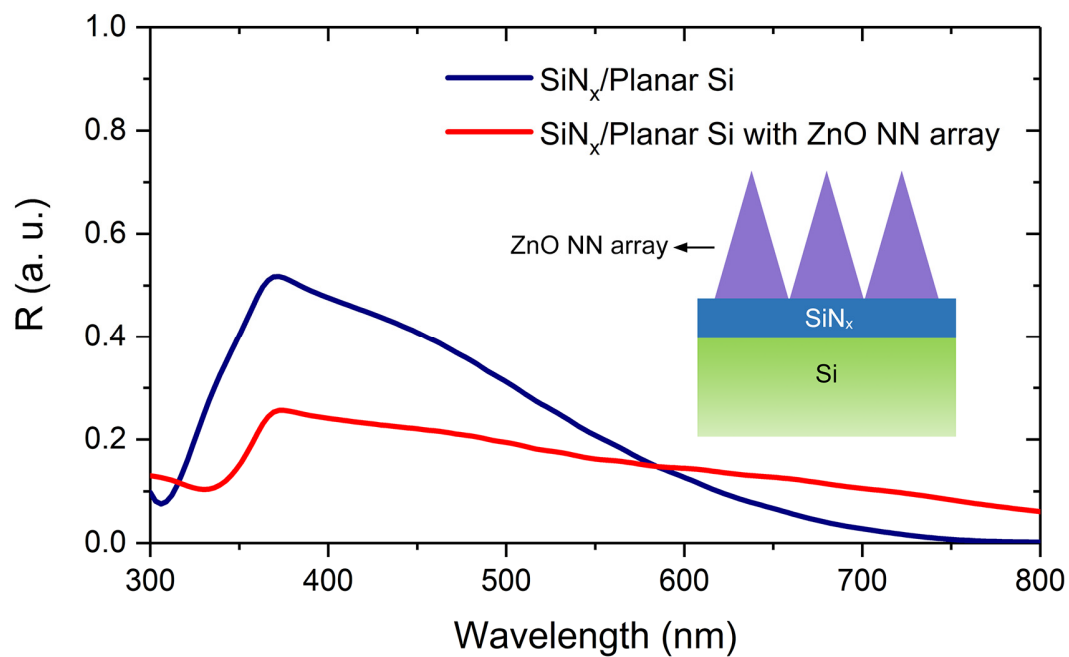


Figure S7. Calculated reflectance for the SiN_x/planar Si with and without ZnO nanoneedle array. The height, diameter, and period are 230 nm, 50 nm, and 50 nm, respectively. The thickness of the SiN_x film is 100 nm. The inset shows the calculated structure.

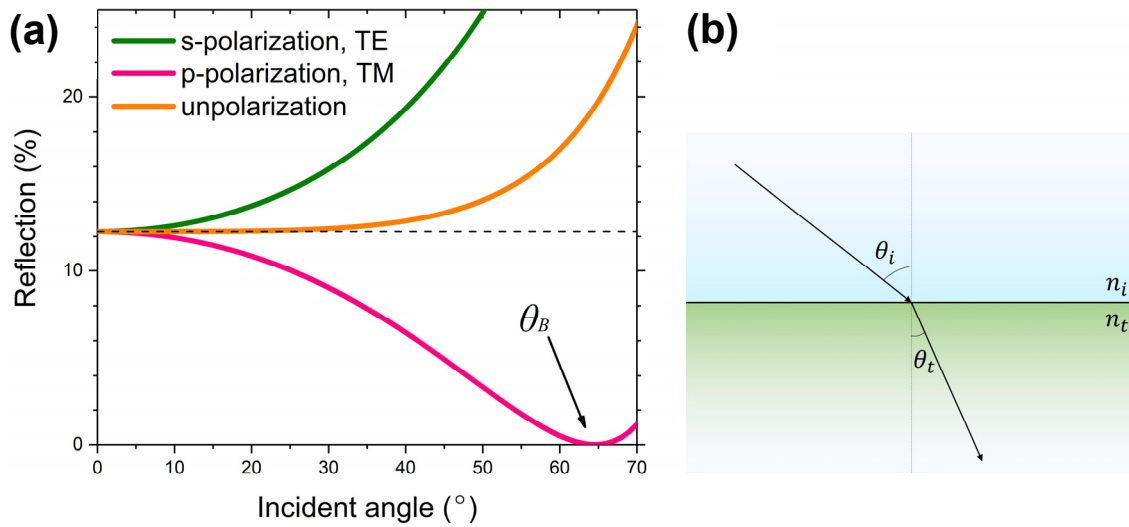


Figure S8. (a and b) Calculated incident-angle-dependent reflection (a) for polarized and unpolarized light at the wavelength of 450 nm using Fresnel equations (The details are explained in section 5 below.). θ_B is Brewster angle at the interface between air and silicon nitride ($n_{i(air)} = 1$, $n_{t(silicon\ nitride)} = 2.07$, and $\theta_B = \tan^{-1}\left(\frac{n_t}{n_i}\right) = 64.3^\circ$) [4]. The dashed line indicates the guideline to show the reflection value at normal incidence. (b) A schematic image showing the incident and transmitted waves through the interface of two media. n_i and n_t are the refractive indices of the incident and transmitted medium, respectively. θ_i and θ_t are the incident and transmitted angles, respectively.

5. Fresnel equation for polarized and unpolarized light

The TE-polarized light is characterized by E-field is perpendicular to the plane of incidence, whereas E-field of TM-polarized light is parallel to the plane of incidence. At the interface between two media which have a different refractive index, the reflection for polarized and unpolarized light is as follow [4].

For TE-polarized light, the reflection becomes

$$R_{TE} = \left| \frac{n_i \cos \theta_i - n_t \cos \theta_t}{n_i \cos \theta_i + n_t \cos \theta_t} \right|^2.$$

where n_i and n_t are the refractive index and θ_i and θ_t are the incident and transmitted angles of the incident and transmitted medium, respectively.

For TM-polarized light, the reflection becomes

$$R_{TM} = \left| \frac{n_t \cos \theta_i - n_i \cos \theta_t}{n_i \cos \theta_t + n_t \cos \theta_i} \right|^2.$$

The reflection for unpolarized light is

$$R_{unpol.} = \frac{R_{TE} + R_{TM}}{2}.$$

References

- [1] Refractive Index Library, Materials: ZnO, <https://www.pvlighthouse.com.au/ko/refractive-index-library>, accessed August 2021, PV Lighthouse.
- [2] K. L. Foo, U. Hashim, K. Muhammad and C. H. Voon, *Nanoscale Research Letters*, 2014, **9**, 429.
- [3] Y. J. Lee, T. L. Sounart, J. Liu, E. D. Spoerke, B. B. Mckenzie, J. W. P. Hsu, and J. A. Voigt, *Crystal growth & Design*, 2008, **8**, 2036-2040.
- [4] E. Hecht, *Optics*, Pearson, 5th edition, 2017.